SSRG International Journal of Mechanical Engineering
ISSN: 2348-8360/ https://doi.org/10.14445/23488360/IJME-V13I11P104

Volume 13 Issue 11, 34-48, November 2026
© 2026 Seventh Sense Research Group®

Original Article

Engineering Design, Structural Validation, and Process Characterization of a PLC-Controlled Recycled PET Filament Extruder for Sustainable Circular Manufacturing

Wirote Ritthong[1,2], Kittigorn Chalernphon[3], Naphat Albutt[3], Wipawadee Wongsuwan[4], Maximiliano Asís-López[5], Khongdet Phasinam[1,6*]

[1]*Faculty of Engineering and Technology, Shinawatra University, Pathum Thani, Thailand.*
[2]*INTI International University, Negeri Sembilan, Malaysia.*
[3]*Faculty of Engineering, Bangkok Thonburi University, Bangkok, Thailand.*
[4]*Faculty of Engineering, Thai-Nichi Institute of Technology, Bangkok, Thailand.*
[5]*Faculty of Science, Universidad Nacional Santiago Antúnez de Mayolo, Huaraz, Peru.*
[6]*Faculty of Engineering and Technology, Pathumthani University, Pathum Thani, Thailand.*

[*]*Corresponding Author: khongdet.p@siu.ac.th*

Received: 21 August 2026 Revised: 21 November 2026 Accepted: 25 November 2026 Published: 27 November 2026

Abstract *- 350 million metric tons of plastic are produced in a year worldwide, making plastic waste management a global concern. In this work, a recycled plastic extruder machine is designed, fabricated, and its systematic performance is evaluated for converting post-consumer thermoplastic pellets into continuous filament for additive manufacturing applications. The machine was designed using Computer-Aided Design (CAD) software and structurally validated using Finite Element Analysis (FEA), under static weight and rated-torque loading, to assess the mechanical integrity of the structure under these operating conditions. The machine consists of three major subsystems, i.e. an injection/extrusion unit with a nitride hardened Screw-Barrel assembly, a temperature regulation system using Omron PID controllers with type-K thermocouples and a PLC-based control panel for real-time process monitoring. Experimental tests of the performance were Performed On Poly (Ethylene Terephthalate) (PET) pellets with a maximum diameter of 10 mm, at a fixed drive frequency of 30 Hz and nozzle temperature of 210°C. After excluding one transient trial recorded immediately after warm-up, the prototype achieved a steady-state extrusion speed of 366.0 ± 23.1 cm min⁻¹ (CV = 6.3%) and a steady-state filament diameter of 1.46 ± 0.21 mm, below the 1.75 mm nozzle and FDM target. A separate motor frequency-speed characterization showed a strongly linear relationship between the drive frequency (10-50 Hz) and screw rotational speed (1.22-6.49 RPM). The prototype demonstrates a promising, low-cost pathway for small-scale plastic recycling and circular economy implementation. The findings contribute to an increasing knowledge of decentralized plastic upcycling technologies and provide a preliminary engineering basis for future scale-up, closed-loop dimensional control, and more rigorous process optimization studies.*

Keywords *- Plastic extrusion, Finite Element Analysis, PLC control, Circular economy, Process characterization.*

1. Introduction

The rapid increase in plastic production throughout the world has become one of the most important environmental problems of the twenty-first century. In the last 70 years, plastic manufacture has increased enormously due to the relatively low cost of production, light weight, durability and versatility of plastic in industrial, commercial and domestic uses. However, this unprecedented growth has been paralleled by an equally rapid accumulation of plastic waste that outpaces the capacity of existing waste-management systems. The total global production of plastics since 1950 has been estimated at about 8300 million metric tons, of which only about 9% has been recycled, 12% incinerated, and almost 79% has been discarded to landfills or released into the natural environment [1].

The Organization for Economic Co-operation and Development (OECD) further estimates that some 400 million metric tons of plastic waste are produced annually worldwide, and this number is expected to almost triple by 2060 without major improvements in waste management

This is an open access article under the CC BY-NC-ND license (http://creativecommons.org/licenses/by-nc-nd/4.0/)

policies and recycling infrastructure [2]. In addition, it is estimated that 4.8 to 12.7 million metric tons of plastic are annually released into marine environments from land-based sources alone, endangering aquatic ecosystems, biodiversity and human health [3]. Besides the visible environmental pollution, the entire life cycle of plastics (from fossil resource extraction, polymer production and consumption to end-of-life degradation) is a major contributor to greenhouse-gas emissions and the global distribution of microplastics in terrestrial ecosystems, marine sediments and food chains [4]. The issue of plastic waste is especially acute in fast-urbanizing countries where economic growth and rising demand for consumer products have outstripped waste-management capacity. Thailand is one of the largest plastic waste-generating countries in Asia, generating approximately 2 to 3.4 million metric tons of plastic waste per year [5, 6]. During high commercial activity, Bangkok, the country's largest metropolitan area, generates over 3,400 metric tons of plastic waste per day, with plastic being the second largest component of municipal solid waste after organic waste [5]. However, despite the existence of the National Roadmap on Plastic Waste Management (2018-2030) in Thailand, material-flow analyses continue to indicate that a large fraction of plastic waste does not enter formal recycling channels, but is instead disposed of by landfilling, open burning or leakage into rivers and coastal environments [6, 7]. Moreover, contaminated or mixed plastic fractions are still especially difficult to recycle efficiently, leading to important losses of material value and limiting the environmental benefits that could be obtained through effective resource recovery and source separation [8]. Thermoplastic Polymers such as Poly (Ethylene Terephthalate) (PET), High-Density Polyethylene (HDPE) and Polypropylene (PP) are of particular interest for mechanical recycling among the different types of plastic waste because they can be melted and re-molded many times without being completely chemically transformed [9, 10]. Mechanical recycling generally requires much less energy than the production of virgin polymer and is therefore an important strategy to reduce carbon emissions and dependence on fossil-derived raw materials [11]. Nevertheless, the polymers are inevitably subjected to thermal, thermo-oxidative and mechanical degradation during repeated melt processing, resulting in chain scission, changes in crystallinity, lower molecular weight and lower melt viscosity. With the increase of extrusion cycles, the mechanical properties and the processing stability of recycled materials gradually degrade due to these degradation mechanisms [12]. Moreover, traditional industrial recycling systems are normally based on costly centralized plants, complex sorting processes, and relatively homogeneous feedstock, which make them economically infeasible for small communities, schools, informal recycling sectors, and resource-poor regions [13, 14]. A decentralized plastic recycling approach has emerged as a promising engineering solution to address these limitations by enabling the conversion of post-consumer plastic waste into value-added products at the local level. Recent studies on waste-derived engineering materials have demonstrated that recycling can provide not only environmental benefits but also economic value through reduced resource consumption, lower lifecycle costs, and carbon-emission mitigation [15]. One of the most interesting applications is the production of filament for Fused Deposition Modeling (FDM) additive manufacturing, which allows to bring discarded plastics back into the production cycle, supporting at the same time circular economy principles and distributed manufacturing [16, 17]. This localized recycling approach reduces the need for transportation, reduces material losses, and reduces reliance on virgin petrochemical resources while opening up new opportunities for community-based manufacturing and educational innovation [13, 18]. Recently, a number of low-cost and open-source desktop extrusion systems have been developed to convert shredded or pelletized plastic waste to printable filament [19], but consistent filament quality remains a major engineering challenge. Commercial FDM printers usually require the filament diameter to be within ±0.05 mm of the nominal 1.75 mm specification to ensure reliable feeding of the material, prevent nozzle clogging and maintain dimensional accuracy during printing [20].

Plastic extrusion is essentially a continuous thermomechanical manufacturing process in which polymer pellets or recycled flakes are transported, melted, compressed and forced through a forming die to produce a product with a constant cross-sectional geometry. The quality of the extruded filament depends on the intricate relationship between the temperature distribution in the barrel, screw geometry, screw speed, residence time, and die pressure [21, 22]. Insufficient control of any of these parameters can lead to incomplete melting, thermal degradation, unstable flow behavior or dimensional variation, which will ultimately reduce the quality and usability of the recycled filament [12, 23]. Thus, an optimized mechanical structure as well as reliable thermal regulation and process control are required for successful development of a compact extrusion system. Modern engineering design methods increasingly include computational analysis and automated control techniques to enhance equipment performance before prototype manufacturing. Finite Element Analysis (FEA) is an effective design tool to assess the structural integrity, stress concentration, deformation prediction and safety of components under operational loading conditions and can reduce the development cost and shorten the design iterations [24, 25]. At the same time, closed-loop temperature control using Programmable Logic Controllers (PLCs) and PID control algorithms can control barrel temperature more precisely, provide stable heating, fault detection and user-friendly operation of the machine, all necessary for consistent polymer processing conditions [26]. The integrated mechanical design, structural performance, thermal control, and operational characteristics of compact

plastic extruders specifically designed for recycled thermoplastic feedstock have not been rigorously evaluated in controlled laboratory conditions, despite the growing interest in open-source recycling technologies [27, 28]. Also, the quantitative relations between the extrusion speed, filament dimensional stability, motor operating frequency, screw rotational speed, and processing temperature are not well reported, so the validated engineering guidelines for decentralized recycling applications are not so well available [27, 28].

We present the full engineering design, fabrication, structural verification and experimental evaluation of a prototype plastic extruder for decentralized recycling of thermoplastic waste. The proposed system comprises a structurally optimized frame, validated by Finite Element Analysis under representative static and rated-torque loading, an Omron PID-based temperature control system, and a Sumitomo gear-motor drive to achieve stable extrusion performance. Four systematic experimental studies were conducted: (i) characterization of extrusion speed under fixed operating conditions, (ii) evaluation of filament dimensions, (iii) correlation of motor frequency with screw rotation speed, and (iv) qualitative screening of nozzle temperature for PET processing. The purpose of the study is: (1) to develop and structurally assess a plastic-recycling extruder through FEA; (2) to construct a working lab-scale prototype; (3) to measure its main operating characteristics under fixed and varied conditions; and (4) to provide a preliminary engineering basis for decentralized plastic upcycling and sustainable resource management in low-resource settings, to be refined through more rigorous statistical optimization in future work.

This study contributes directly to the United Nations Sustainable Development Goals (SDGs), particularly SDG 9 (Industry, Innovation and Infrastructure) through engineering innovation, SDG 12 (Responsible Consumption and Production) by promoting decentralized plastic recycling and circular manufacturing, and SDG 13 (Climate Action) through resource-efficient utilization of recycled PET feedstock and reduction of plastic waste.

2. Materials and Methods

2.1. Feedstock Materials

The extrusion feedstock for all experiments was Post-Consumer Poly (Ethylene Terephthalate) (PET) pellets. The pellets, nominally less than 10 mm maximum particle size, were supplied by a certified plastic recycling facility that processes post-consumer beverage bottles collected through municipal solid-waste segregation programs. PET (resin identification code 1, ASTM D7611) was chosen based on its availability in Post-Consumer Recycling (PCR) streams, known melt-processing properties, moderate processing temperatures and proven suitability for the production of Fused Deposition Modeling (FDM) filaments (Table 1). The use of recycled PET also supports circular economy principles by taking plastic waste out of landfills and returning discarded materials to productive manufacturing uses. The pellets were characterized before extrusion to define baseline material properties and to verify feedstock consistency. In accordance with ASTM D4603, Intrinsic Viscosity (IV) was determined to be 0.72 ± 0.03 dL g^{-1} using a phenol/tetrachloroethane (60:40) solvent system at 30°C, which suggests a molecular weight suitable for extrusion-grade PET and adequate melt strength in the filament drawing process. The Melt Flow Index (MFI) was determined according to ISO 1133 at 265 °C with a 2.16 kg load and was 18 ± 2 g/10 min, confirming suitable melt flow for single-screw extrusion. The bulk density of the pellets was 820 ± 15 kg m^{-3}, and the Differential Scanning Calorimetry (DSC) showed a glass transition temperature (Tg) of 78 ± 1°C, melting temperature (Tm) of 252 ± 2°C and an initial crystallinity of 28 ± 3%. The main physical and thermal properties of the recycled PET feedstock are shown in Table 1.

Table 1. Physical and thermal characterization of the post-consumer PET pellet feedstock

Property	Value	Test Method
Intrinsic Viscosity (IV)	0.72 ± 0.03 dL/g	ASTM D4603
Melt flow index (265°C/2.16 kg)	18 ± 2 g/10 min	ISO 1133
Bulk density	820 ± 15 kg/m³	Volumetric method
Glass transition temperature (Tg)	78 ± 1°C	DSC, ISO 11357-2
Melting temperature (Tm)	252 ± 2°C	DSC, ISO 11357-3
Crystallinity (as-received)	28 ± 3%	DSC
Nominal particle size (max)	≤10 mm	Sieve analysis

Moisture control was identified as a critical pre-processing step because PET is very sensitive to hydrolytic degradation at melt-processing temperatures. Residual moisture facilitates ester bond cleavage, resulting in molecular weight reduction and increased melt flow, deterioration of mechanical properties, and formation of volatile degradation products negatively affecting the filament quality. For reduction of these effects, the pellets were dried at 80°C for 4 h in a forced-convection oven (Memmert UN55, Germany) following industrial established recommendations. Moisture content was determined by moisture analyzer (Ohaus MB120, resolution 0.001%) before and after drying. The as-received pellets had initial moisture contents ranging from 0.18 to 0.25 wt%, but the drying

process reduced the moisture level to less than 0.015 wt% following the recommended specification for extrusion-grade PET. The pellets were sealed immediately in moisture-resistant polyethylene bags and transferred directly to the extruder hopper immediately after drying to minimize moisture reabsorption prior to processing. This procedure ensured uniform feedstock quality in all experimental investigations.

2.2. Design of Machines and Structural Analysis

The prototype plastic extruder was developed as a lab-scale recycling platform comprising three major subsystems, namely, an extrusion unit, a PID-based temperature control system, and a variable-speed drive system, mounted on a welded mild-steel structural frame (SS400 grade) with overall dimensions of 104 × 100 × 130 cm (L × W × H), as shown in Figure 1(a). The rigid frame was built to give sufficient structural rigidity to hold the barrel assembly, drive motor, hopper, and control components with a minimum of vibration during continuous operation. The mechanical design was finalized in SolidWorks® 2023 (Dassault Systèmes, France), and structural integrity was verified with static Finite Element Analysis (FEA) prior to fabrication. Critical load-bearing components such as the frame members, barrel-support brackets, motor mounting plates and welded joints were tested under combined static and operational loading conditions.

The applied loading was the distributed weight of the screw-barrel assembly and a dynamic motor torque of 47 N·m at 50 Hz inverter operation; thermal expansion stresses, start-up/impact loading, weld fatigue under cyclic operation, and the temperature-dependent reduction in SS400 yield strength at elevated barrel-zone temperatures were not included in the present model and are identified as limitations of the current structural assessment. The four adjustable leveling feet were fixed support boundary conditions, and the reaction forces from the simulation were used to verify weld dimensions against AWS D1.1 design requirements. The extrusion system was a nitrided steel single screw with an outer diameter of 25 mm and an L/D ratio of 18.8, as shown in Figure 1(b). The screw geometry was divided into three functional sections: a feed zone (40% of the total screw length) for conveying solid material, a transition zone (30%) for progressive melting and a metering zone (30%) for melt homogenization and pressure stabilization prior to extrusion. The nitrided barrel with an internal diameter of 25 mm was supported concentrically with ceramic heating bands and barrel-support brackets as shown in Figure 1(d). An open-type converging nozzle with a 1.75 mm exit diameter was selected to produce FDM-compatible filament (Figure 1(c)). A 1.1 kW Sumitomo helical gear motor, coupled with a 1:83 reduction gearbox, drove the screw. A variable-frequency drive (10-50 Hz) enabled continuous speed adjustment in the range of 1.22-6.49 rpm. The theoretical volumetric throughput was estimated from the continuity relationship, $Q = A \times V$, where A is the effective screw-channel cross-sectional area, and V is the mean axial melt velocity. The integrated mechanical design offers a structurally robust and operationally stable platform for the assessment of recycled PET extrusion under controlled laboratory conditions.

2.3. Temperature Control and Transfer Apparatus

Stable thermal control and regulated screw rotation are essential for consistent polymer melting and dimensional stability during filament extrusion. To this end, the prototype extruder included an integrated temperature-control and power-transmission system intended to provide precise thermal management and smooth mechanical operation during the extrusion process. The barrel heating system was a two-zone temperature-control system with Omron E5CC-QX2ASM-800 PID controllers (Omron Corporation, Japan). Independent temperature control of the feed and metering sections allowed localized heat distribution according to the thermal requirements of individual processing zones. The nozzle temperature was monitored by Type-K thermocouples (accuracy ±1.5°C), and the barrel temperature was continuously measured by a PT100 Resistance Temperature Detector (RTD) (accuracy ±0.3°C). Thermal stability during continuous extrusion was achieved by using closed-loop PID control that automatically adjusted the heater output based on real-time sensor feedback, minimizing temperature variations. The necessary heating energy was provided by ceramic band heaters (220 V AC, 300 W per zone), and power switching was performed by Siemens 3RT series magnetic contactors. The entire control system was integrated with a 24 V DC Programmable Logic Controller (PLC) with digital input/output modules for motor start-stop control, emergency shutdown and indicator-lamp status monitoring, enhancing operational safety and process reliability.

Power for mechanical operation was provided by a helical gear motor, a Sumitomo CNHM02-6095YB-11 with a rating of 1.1 kW, running from a 220 V AC, three-phase supply. A 1:83 reduction gearbox was used to transfer the power of the motor to the extrusion screw. This provided the high torque and low rotational speed for stable single-screw extrusion. The rotational speed was continuously controlled by a Variable-Frequency Drive (VFD) with inverter frequencies between 10 and 50 Hz, which corresponded to experimentally validated screw speeds of 1.22-6.49 rpm. The range of speeds was adequate to evaluate the influence of screw rotation on extrusion performance for various processing conditions. The drive shaft was coupled to the screw by a hub-bearing assembly and was supported by tapered roller bearings designed to withstand the combined axial thrust and radial loads developed during continuous operation. Accurate thermal regulation and stable torque transmission provided repeatable operating conditions for all experimental investigations.

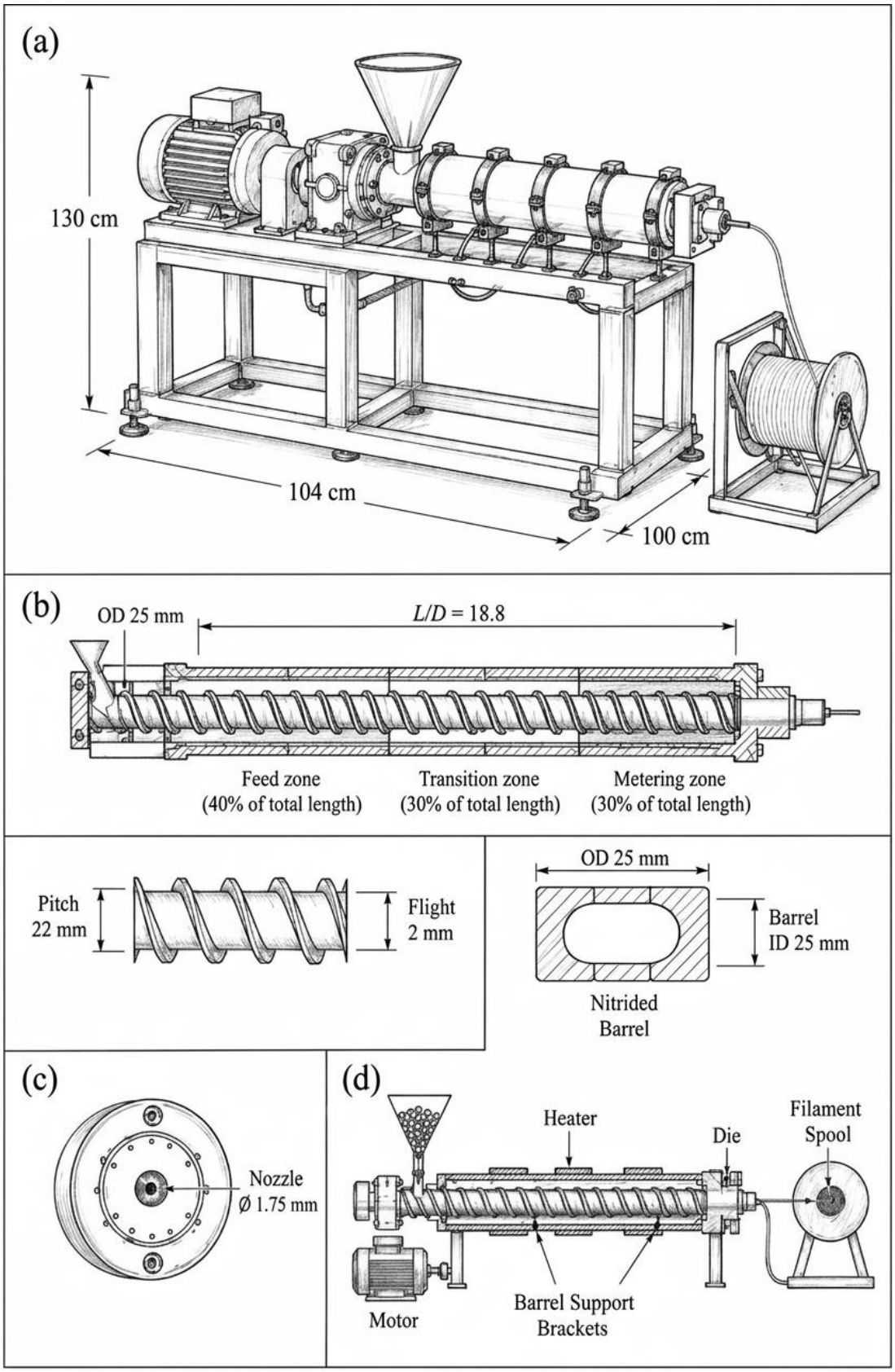


Fig. 1 Engineering configuration of the prototype plastic extruder showing the assembled machine, screw-barrel geometry, extrusion nozzle, and integrated drive system used for structural validation and experimental evaluation.

2.4. Performance Test Protocol

The performance evaluation of the prototype plastic extruder was done experimentally in a steady-state operation after 15 min warm-up period to reach thermal equilibrium in the barrel. Four independent performance tests were performed to evaluate the mechanical and processing characteristics of the extrusion system.

The first experiment was to evaluate the speed of extrusion, which is the production capacity of the machine. Filament was ejected from the nozzle and collected for a fixed time of 60 s at a constant drive frequency of 30 Hz and a nozzle temperature of 210°C. Five independent trials were performed, and the extrusion rate was calculated in cm min^{-1}. Then the process repeatability was calculated in terms of mean value and standard deviation.

The second experiment was designed to evaluate the dimensional consistency of filaments, an important quality parameter for Fused Deposition Modeling (FDM) applications. The diameter of the filament was measured at five equidistant positions along each extrudate using a digital vernier caliper with a resolution of 0.01 mm. The total filament length produced in each trial was also recorded. The measurements were repeated on five specimens, and the mean values with their standard deviations were calculated.

The third experiment was performed to study the relation between the motor drive frequency and the screw rotational speed. The inverter frequency was changed incrementally from 10 to 50 Hz with an increment of 10 Hz, and the corresponding screw speed was measured with a non-contact digital tachometer with an accuracy of ±1 rpm. The operating characteristics of the transmission system were checked using the obtained frequency-speed relation.

Finally, the effect of processing temperature was screened by testing nozzle temperatures of 180, 190, 200, 210, and 220°C, with the barrel temperature maintained 20°C below the nozzle temperature. All conditions were run at a fixed extrusion cycle time of 5 s.

The quality of the extrudate was evaluated by two trained operators independently using a standardized three-level classification: Not Acceptable, Acceptable and Good, based on surface aspect, diameter uniformity and absence of visible defects such as voids, incomplete melting or discoloration. This temperature screening was exploratory in nature, based on descriptive statistics and qualitative visual scoring rather than a randomized factorial design, and should be interpreted as an empirical operating-condition screening rather than a validated optimization. Combined, these experiments give a preliminary assessment of the extrusion system in terms of productivity, dimensional accuracy, mechanical performance, and processing stability.

2.5. Statistical Analyses

All experimental measurements were analyzed using descriptive statistical methods to evaluate the repeatability and consistency of the prototype plastic extruder under identical operating conditions. Data processing was performed using Microsoft Excel 2021, and all quantitative results are presented as the mean ± Standard Deviation (SD) based on five independent experimental replicates. The use of descriptive statistics provides a straightforward assessment of process variability while enabling direct comparison among the evaluated extrusion performance parameters. For filament dimensional quality, the Coefficient of Variation (CV%) was additionally calculated to assess diameter uniformity, which is a critical requirement for Fused Deposition Modeling (FDM) filament production. The CV expresses the relative variability of the measured filament diameter with respect to its mean value, allowing dimensional consistency to be evaluated independently of the nominal diameter. Lower CV values indicate more stable extrusion behavior and improved process repeatability. All experiments were conducted during a single laboratory session under controlled environmental conditions with an ambient temperature of 28 ± 2°C, thereby minimizing the influence of external temperature fluctuations on extrusion performance. Processing conditions, measurement procedures, and instrument settings were maintained constant throughout all experimental trials to ensure experimental consistency and reduce systematic variation. It should be noted that all statistical treatment in this study is limited to descriptive measures (mean, SD, CV); no randomized experimental design, factorial analysis, ANOVA, response-surface methodology, or independent replication across separate laboratory sessions was performed. Consequently, the present results should be interpreted as prototype characterization and preliminary parameter screening rather than a statistically validated process optimization, and the coupled effects of screw speed, temperature, feeding, and downstream drawing conditions were not jointly optimized.

Extrusion speed, filament length and filament diameter results for the five repeated trials conducted at a fixed drive frequency of 30 Hz and nozzle temperature of 210°C are summarized in Tables 3 and 4 (Sections 3.2 and 3.3). The independently measured relationship between inverter drive frequency (10-50 Hz) and screw rotational speed is reported separately in Table 5 (Section 3.4). These datasets provide the basis for evaluating the overall operational stability of the prototype extruder and serve as reference data for the subsequent analysis of extrusion performance.

3. Results and Discussion

3.1. Finite Element Analysis (Structural Analysis)

The structural performance of the proposed plastic extruder was evaluated through a mesh-convergence study and a static Finite Element Analysis (FEA) under the static and rated-torque loading described in Section 2.2. The

convergence results presented in Figure 2 indicate that the predicted von Mises stresses were virtually mesh-independent for a global element size of 5 mm. Refinement from 5 to 15 mm caused only small changes in stress at all critical locations, confirming numerical convergence and ensuring that the chosen mesh density provided a proper compromise between computational efficiency and solution accuracy. The low coefficients of variation (CV = 2.9-7.1%) also suggest very good numerical stability and repeatability over the convergence analysis (Table 2). Of the structural components tested, the barrel support bracket had the highest von Mises stress (48.3 ± 1.4 MPa), followed by the motor mounting pad (31.6 ± 1.1 MPa), with relatively low stress in the frame base leg (22.4 ± 0.9 MPa) and distal barrel end (12.7 ± 0.8 MPa) (Table 2). The stress distribution is in good agreement with the mechanical loading configuration of the machine where the barrel support bracket is loaded by the combined effects of the cantilevered screw-barrel assembly and the transmitted motor torque. The concentration of stress at this location therefore is indicative of the primary structural load path and not a localized design weakness. Despite these localized stress concentrations, the predicted stress values were all well below the yield strength of SS400 structural steel (245 MPa), resulting in safety factors between 5.07±0.15 and 19.3±1.2 (Table 2).

They are significantly higher than the minimum design requirements normally used for welded industrial machinery, which implies a significant structural safety margin for the static and rated-torque loading conditions considered. Moreover, the predicted maximum displacement was only 0.42 ± 0.03 mm at the distal barrel end with the largest unsupported overhang and negligible at the frame base (0.05 ± 0.01 mm) (Table 2). The predicted frame deformation is unlikely to impact shaft alignment or extrusion performance, given the typical operational barrel-screw radial clearance of 0.10-0.30 mm. In general, the FEA results show that the proposed structural configuration is sufficiently stiff and strong for the loading conditions modeled.

The mesh-independent numerical solution (Figure 2) and high safety factors (Table 2) give good engineering evidence for this baseline structural assessment; however, as noted in Section 2.2, thermal stress, start-up/impact loading, weld fatigue and the temperature-dependent reduction in SS400 strength were outside the scope of the present static model, so the reported safety factors should be regarded as indicative under normal steady-state operation rather than a comprehensive structural validation across all service conditions.

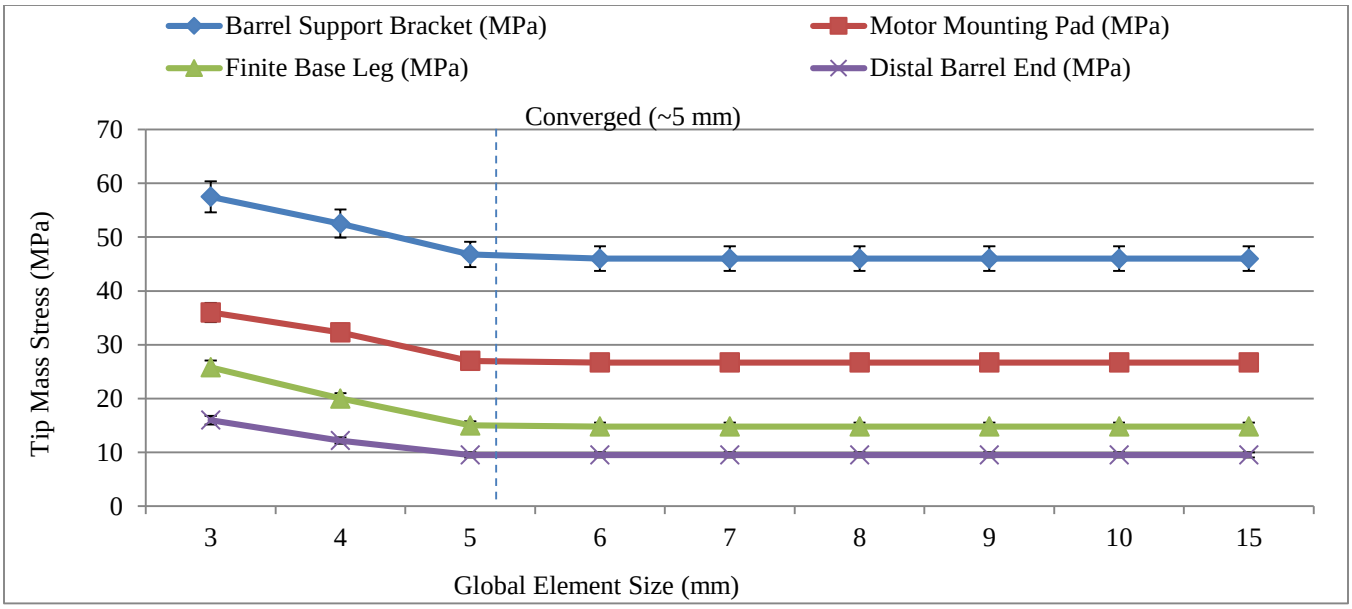


Fig. 2 Mesh-Convergence analysis of the finite element model showing von Mises stress at four critical structural locations. A 5 mm global element size achieved solution convergence and was adopted for subsequent structural simulations.

Table 2. FEA-Derived von Mises stress, maximum displacement, and structural safety factors at critical frame locations under the static weight and rated-torque loading described in Section 2.2 (Mean ± 1 SD, n = 5 mesh-sensitivity trials). Thermal stress, impact/start-up loading, weld fatigue, and elevated-temperature strength reduction of SS400 were not included in this model (see Section 2.2).

Location	Von Mises Stress (MPa)	Displacement (mm)	Safety Factor (SF)	CV (%)
Barrel support bracket	48.3 ± 1.4	0.18 ± 0.02	5.07 ± 0.15	2.9
Motor mounting pad	31.6 ± 1.1	0.09 ± 0.01	7.75 ± 0.27	3.5
Distal barrel end	12.7 ± 0.8	0.42 ± 0.03	19.3 ± 1.2	7.1
Frame base leg (max.)	22.4 ± 0.9	0.05 ± 0.01	10.9 ± 0.4	4.0

CV = Coefficient of Variation; SF = Safety Factor relative to SS400 yield strength (245 MPa).

3.2. Performance of Extrusion Velocity

Five consecutive trials were conducted at the same fixed operating condition (30 Hz drive frequency, 210°C nozzle temperature) to assess the repeatability of the prototype extruder, and the results are summarized in Table 3 and presented in Figure 3. The average extrusion speed for all trials combined was 406.6 ± 89.9 cm min^{-1} (CV = 22.1%), suggesting a relatively high variability in production rate. This variability was driven almost entirely by Trial 2, which showed a markedly higher extrusion speed (569 ± 35 cm min^{-1}) than the other four trials (Figure 3). Because Trial 2 was run after the same 15-minute thermal warm-up as Trial 1, the excursion cannot be attributed solely to residual thermal non-equilibrium; plausible contributing factors include a transient pressure fluctuation in the barrel, localized voiding or incomplete compaction of the feedstock, or an isolated measurement artifact, but the present dataset does not allow the exact cause to be established with confidence. Excluding Trial 2, the extrusion speed for Trials 1, 3, 4 and 5 was 366.0 ± 23.1 cm min^{-1}, with a substantially lower CV of 6.3% (Table 3). The reduced variability among these four trials indicates that the extrusion system is capable of consistent melt transport and screw conveying performance under steady operation; however, because the cause of the Trial 2 excursion was not conclusively identified, this interpretation should be confirmed with additional replicated trials, ideally across multiple laboratory sessions, in future work. From an engineering perspective, the steady-state extrusion rate is on the order of ~220 m h^{-1}, which is lower than the production capacity of commercial industrial extrusion systems, but fits in well with laboratory-scale evaluation and decentralized recycling applications. Most importantly, the low steady-state variability indicates that the combined effects of screw geometry, PID-based temperature control, and variable-frequency drive were successful in maintaining stable extrusion conditions during continuous operation. The ability to generate repeatable extrusion rates is especially important for recycled PET as fluctuations in melt throughput directly affect the filament diameter and dimensional uniformity during downstream cooling and winding. Overall, the results show that the prototype extruder achieves stable and repeatable material throughput once steady state processing is reached, provided that trials such as Trial 2 are recognized and investigated rather than excluded. This emphasizes the need for a suitable stabilization protocol and additional replication before performance or filament manufacturing is evaluated. Thus, the extrusion system shows promising operational reliability for small-scale recycled PET processing and is a suitable platform for further investigations of the dimensional accuracy of the filament and more rigorous, statistically designed process optimization in future work.

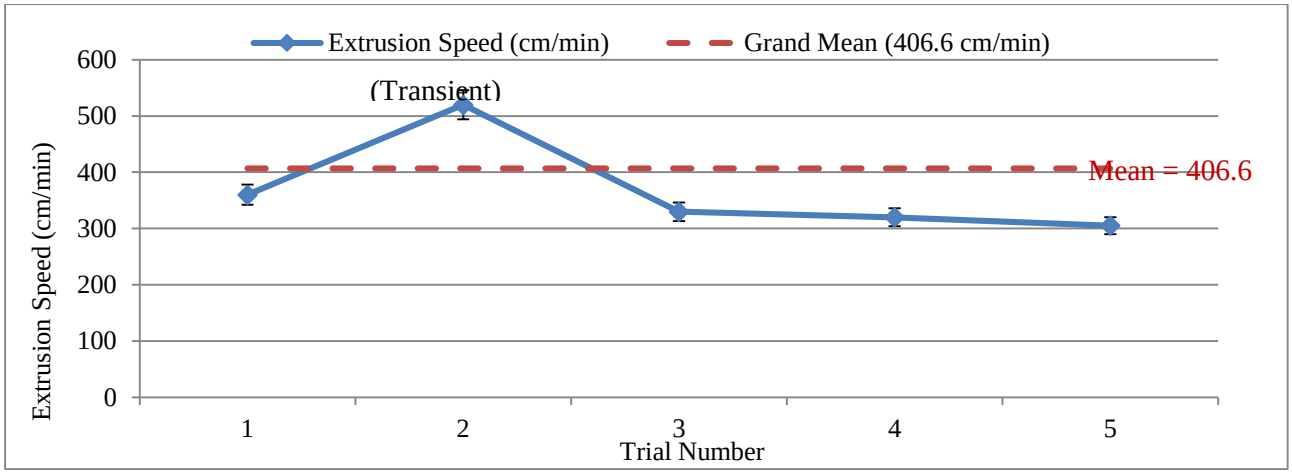


Fig. 3 Trial-by-Trial extrusion speed of the prototype plastic extruder under identical operating conditions. Error bars indicate ±1 SD (n = 5), and the dashed line represents the overall mean extrusion speed of 406.6 cm/min.

Table 3. Trial-by-Trial extrusion speed, filament length, and filament diameter recorded at a fixed 30 Hz drive frequency and 210°C nozzle temperature (Mean ± 1 SD; n = 5 per trial; *Trial 2 identified as an excursion of undetermined cause, see Section 3.2).

Trial	Extrusion Speed (cm/min)	Filament Length (cm)	Diameter (mm)	Note
1	395 ± 22	395 ± 12	1.15 ± 0.06	Steady-state
2	569 ± 35*	569 ± 21*	0.90 ± 0.08*	Transient surge
3	369 ± 19	369 ± 11	1.65 ± 0.07	Steady-state
4	359 ± 18	351 ± 10	1.55 ± 0.06	Steady-state
5	341 ± 17	341 ± 10	1.50 ± 0.06	Steady-state
All trials mean ± SD	406.6 ± 89.9	405.0 ± 90.7	1.35 ± 0.28	CV = 22.1%
Trials 1,3-5 mean ± SD	366.0 ± 23.1	364.0 ± 24.0	1.46 ± 0.21	CV = 6.3%

CV = Coefficient of Variation. Shaded row (Trial 2) denotes the trial with an unexplained speed/diameter excursion, excluded from the steady-state summary statistics (see Section 3.2 for discussion of possible causes).

3.3. Filament Dimensional Characteristics

The dimensional characteristics of the extruded PET filament were evaluated by measuring filament diameter and extrudate length over the same five consecutive trials described in Section 3.2. The experimental results are summarized in Table 4 and illustrated in Figure 4. Across all measurements, the average filament diameter was 1.35 ± 0.28 mm, corresponding to an overall Coefficient of Variation (CV) of 20.7%. This relatively high variability was primarily associated with Trial 2, where the filament diameter decreased to 0.90 ± 0.08 mm, coinciding with the speed/length excursion identified in Section 3.2. The simultaneous increase in extrudate length (569 ± 21 cm) and reduction in filament diameter in that trial is consistent with a temporary increase in material throughput promoting filament draw-down immediately after extrusion, producing a smaller cross-sectional area despite the constant nozzle geometry (Figure 4), although, as noted in Section 3.2, the underlying cause of that trial's behavior was not conclusively established. Excluding Trial 2, filament diameters for Trials 1 and 3-5 ranged from 1.15 to 1.65 mm, with within-trial variability of CV = 3.9-5.2% (Table 4). These results indicate that the combined effects of the screw geometry, temperature regulation, and controlled screw speed provided reasonably repeatable melt flow and filament formation across the remaining trials.

The measured filament diameter remained consistently below the 1.75 mm target nozzle specification across all trials (Figure 4). The average dimensional deficit of 0.40 mm, corresponding to a mean contraction of 22.9% (Table 4), suggests that gravitational draw-down exceeded die-swell recovery under the present processing conditions. This behavior is consistent with the viscoelastic response of recycled PET, where limited melt elasticity and continuous tensile loading during free-span cooling promote filament stretching before solidification. Consequently, the observed dimensional reduction is attributed primarily to insufficient post-extrusion diameter control rather than instability within the extrusion process itself. From an engineering perspective, these findings indicate that the prototype extruder can produce recycled PET filament under the tested conditions; however, downstream dimensional control remains the principal limitation, and the produced filament diameter did not meet the ±0.05 mm commercial FDM tolerance stated in the Introduction. Incorporating a synchronized haul-off mechanism with closed-loop laser diameter feedback would provide continuous regulation of filament tension, reduce draw-down, and improve compliance with the dimensional tolerance required for commercial FDM filament production; no such feedback control was implemented or tested in the present prototype.

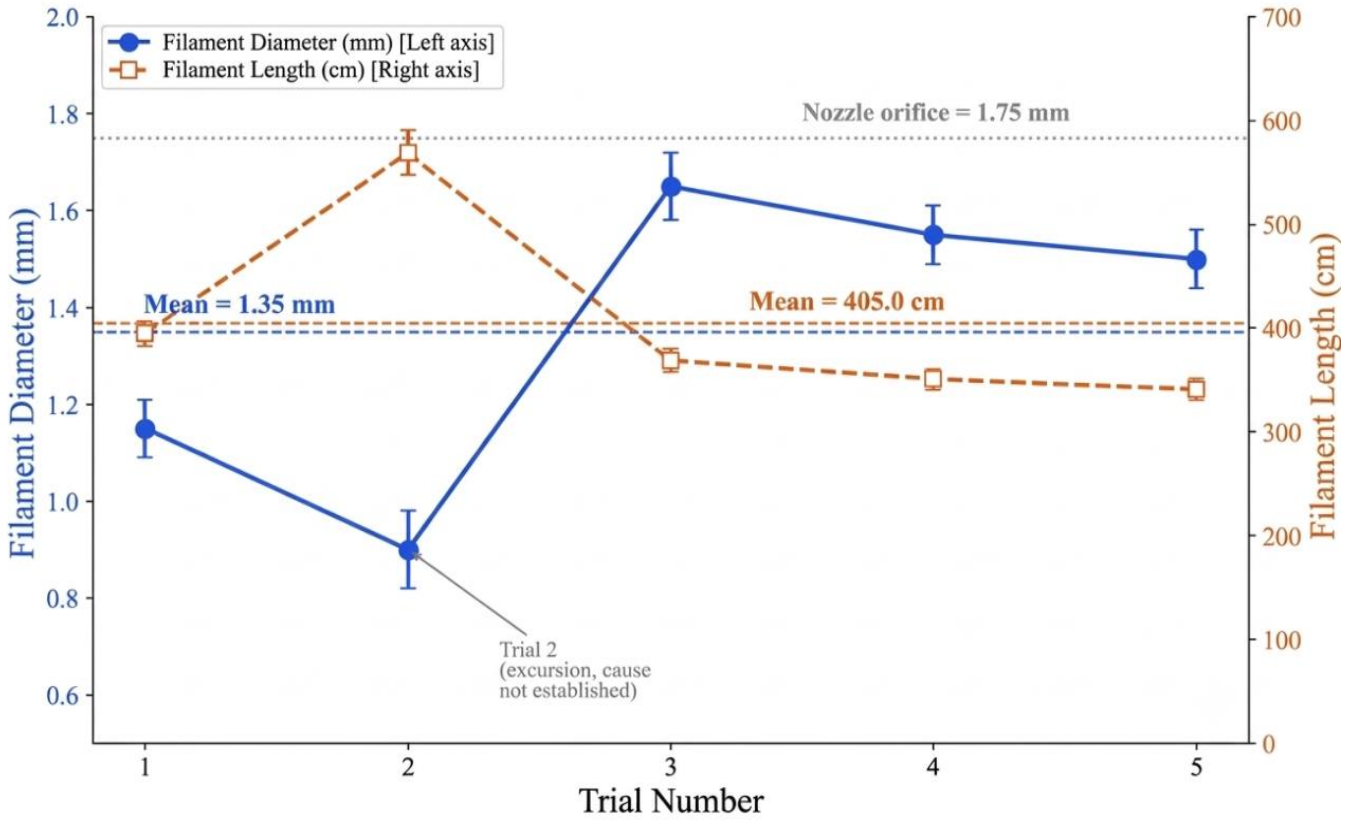


Fig. 4 Trial-by-Trial variation in filament diameter and extrudate length during PET extrusion, regenerated directly from the Table 4 dataset. Error bars indicate ±1 SD (n = 5). The dotted line denotes the 1.75 mm nozzle orifice diameter; dashed lines denote the overall mean filament diameter (1.35 mm) and mean extrudate length (405.0 cm). Trial 2 (Marked) is the excursion trial discussed in Section 3.2.

Table 4. Trial-by-Trial filament diameter and length with die-swell contraction relative to target nozzle orifice (1.75 mm). Values: Mean ± 1 SD (n = 5 measurements per trial).

Trial	Diameter (mm)	Length (cm)	Δd (mm)†	Contraction (%)‡	CV_x (%)
1	1.15 ± 0.06	395 ± 12	−0.60	34.3	5.2
2	0.90 ± 0.08	569 ± 21	−0.85	48.6	8.9
3	1.65 ± 0.07	369 ± 11	−0.10	5.7	4.2
4	1.55 ± 0.06	351 ± 10	−0.20	11.4	3.9
5	1.50 ± 0.06	341 ± 10	−0.25	14.3	4.0
Mean ± SD	1.35 ± 0.28	405.0 ± 90.7	−0.40	22.9	20.7%

†Δd = measured diameter − nozzle orifice diameter (1.75 mm); ‡Contraction (%) = |Δd|/1.75 × 100; CV_x = coefficient of variation of diameter within trial.

3.4. Motor Frequency-Speed Characterization

The relationship between the inverter drive frequency and the measured rotational speed of the screw is plotted in Figure 5. Values are tabulated and compared to theoretical expectations in Table 5. The measured data points (filled circles, Figure 5) showed a remarkable linearity over the entire test range of 10-50 Hz, with the least-squares regression yielding a slope of 0.130 RPM/Hz and an intercept of 0.02 RPM (R^2 = 0.999).

The error bars (±1 SD, n = 5) were narrow at each setpoint and increased modestly from ±0.04 RPM at 10 Hz to ±0.09 RPM at 50 Hz, indicating that the VFD-motor-gearbox assembly produces highly repeatable speed output throughout the constant-torque operating region below base frequency [28]. The dashed regression line in Figure 5 almost overlaps with the measured series, providing a visual confirmation of the near-perfect linearity of the frequency-speed response. The measured speeds were 1.7- 7.8% higher than the theoretical synchronous speeds for the five setpoints (Table 5, Deviation column), which is a consistent positive offset from the inherent slip compensation in the VFD firmware and a small tolerance in the gearbox ratio. Nevertheless, the monotonic near-linear trend of deviation confirms that a single empirical calibration factor is adequate to correct the predicted throughput at any operating frequency.

The estimated extrusion throughput based on the measured screw speed and the screw pitch (22 mm) ranged from ~99 cm/min at 10 Hz to 527 cm/min at 50 Hz (Table 5, rightmost column), providing a 5.3-fold dynamic range to meet the diverse filament diameter and material viscosity requirements.

Such a well-characterized frequency-speed-throughput relationship provides a ready-to-implement lookup table for PLC-based recipe management whereby operators may select a target drive frequency from a stored setpoint library without the need for real-time tachometer feedback [14]. Figure 5 shows the Screw Rotational Speed (RPM) versus VFD drive frequency (Hz) over the 10-50 Hz range.

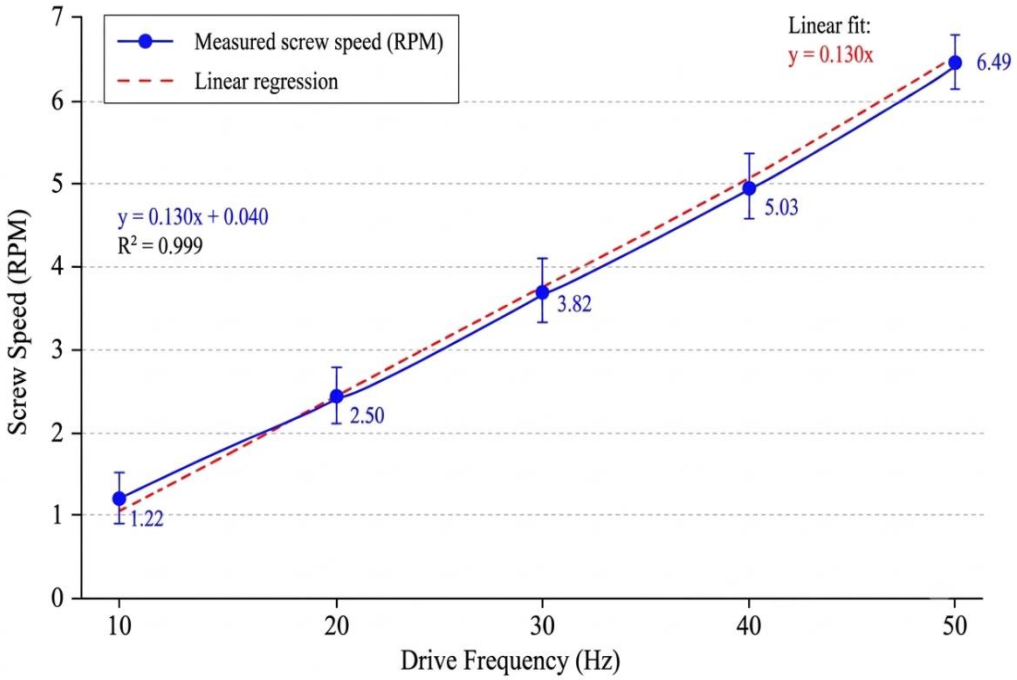


Fig. 5 Relationship between drive frequency and measured screw speed of the prototype extruder. Error bars indicate ±1 SD (n = 5). The dashed line represents the linear regression (R^2 = 0.999), demonstrating excellent speed-control linearity.

Table 5. Measured and theoretical screw speeds at five drive frequencies, with percentage deviation and estimated extrusion throughput (Mean ± 1 SD; n = 5 replicate readings per frequency setpoint). Theoretical speeds were computed from the manufacturer-rated motor synchronous speed; full nameplate parameters (Rated synchronous speed, pole configuration) are available from the corresponding author upon request to allow independent verification of this calculation.

Frequency (Hz)	Measured Speed (RPM, mean ± SD)	Theoretical Speed† (RPM)	Deviation (%)	Est. Throughput‡ (cm/min)
10	1.22 ± 0.04	1.20	+1.7	≈99
20	2.50 ± 0.06	2.41	+3.7	≈203
30	3.82 ± 0.07	3.61	+5.8	≈310
40	5.03 ± 0.08	4.82	+4.4	≈408
50	6.49 ± 0.09	6.02	+7.8	≈527
Slope (RPM/Hz)	0.130	0.120	$R^2 = 0.999$	—

†Theoretical speed = rated motor synchronous speed at 50 Hz × (Hz/50) ÷ gear ratio (83); ‡estimated from measured mean screw speed × pitch (22 mm) × 60 s/min.

3.5. Effect of Nozzle Temperature on Extrudate Quality

Figure 6 shows the effect of nozzle temperature on the extrudate quality score and filament diameter CV. This was an empirical operating-condition screening across five nozzle temperature setpoints (180-220°C) rather than a mechanistic determination of the PET melting and degradation behavior: melt temperature, shear/viscous heating, die pressure, residence time and axial barrel temperature distribution were not independently measured, and extrudate quality was assessed using a subjective three-level visual classification rather than an instrumented measurement.

It is also noted that the DSC-measured melting temperature of the feedstock (Tm = 252 ± 2°C, Table 1) is higher than the nozzle setpoints tested (180-220°C); the present data cannot establish whether the actual melt temperature within the barrel differed from the nozzle setpoint (e.g., due to viscous/shear heating) or whether partial melting/plasticization was sufficient for acceptable extrudate quality at the tested setpoints, and this remains an open question for future work using direct melt-temperature instrumentation. With this scope in mind, both the extrudate quality score and filament diameter CV were strongly setpoint-dependent, indicating that thermal control is one of the most important operating parameters in this system. At 180°C, it was not possible to obtain a continuous filament because the polymer melt was not sufficiently plasticized.

The melt flow of recycled PET was constrained through the die by the incomplete melting, which led to an unstable extrusion and unacceptable product. Increasing the nozzle temperature to 190°C significantly improved the material flow and provided continuous filament formation.

However, the rather large diameter variation indicates that the melt homogenization was not yet finished. This is consistent with local viscosity variations within the polymer melt, with partially molten regions causing unstable flow and irregular filament stretching just after exiting the die (Figure 6). The best extrudate quality scores and lowest filament diameter CV in this screening were observed at nozzle setpoints of 200-210°C (Figure 6). Within the scope of the present qualitative assessment, this setpoint range appears to offer a practical working window for this prototype; confirming it as a genuinely optimal processing condition would require the melt-temperature and material characterization noted above.

Increasing the nozzle temperature setpoint to 220°C was associated with a marked decline in extrudate quality score. Although melt flow remained continuous, the increase in filament diameter CV points to unstable flow behavior. Visual observation also indicated yellowing and the generation of smoke at this setpoint, which are consistent with, but do not on their own confirm, thermo-oxidative degradation of the recycled PET; no post-processing material characterization (e.g., intrinsic viscosity, melt flow index, DSC, TGA, or chemical analysis) was performed to verify polymer chain scission or molecular-weight reduction, and this quantitative confirmation is identified as necessary future work before the 220°C behavior can be attributed definitively to thermal degradation rather than, for example, a purely rheological or processing-related effect.

The practical implication for this prototype is that operation at 220°C produced unacceptable extrudate quality and is therefore not recommended, regardless of the underlying mechanism. In general, the present screening data indicate that nozzle setpoints of 200-210°C gave the best combination of extrusion stability, surface quality and dimensional consistency among the five setpoints tested.

From an engineering standpoint, maintaining the nozzle temperature within this range is advisable for this prototype; further quantitative material characterization is required before this can be generalized as a validated optimum for recycled PET processing.

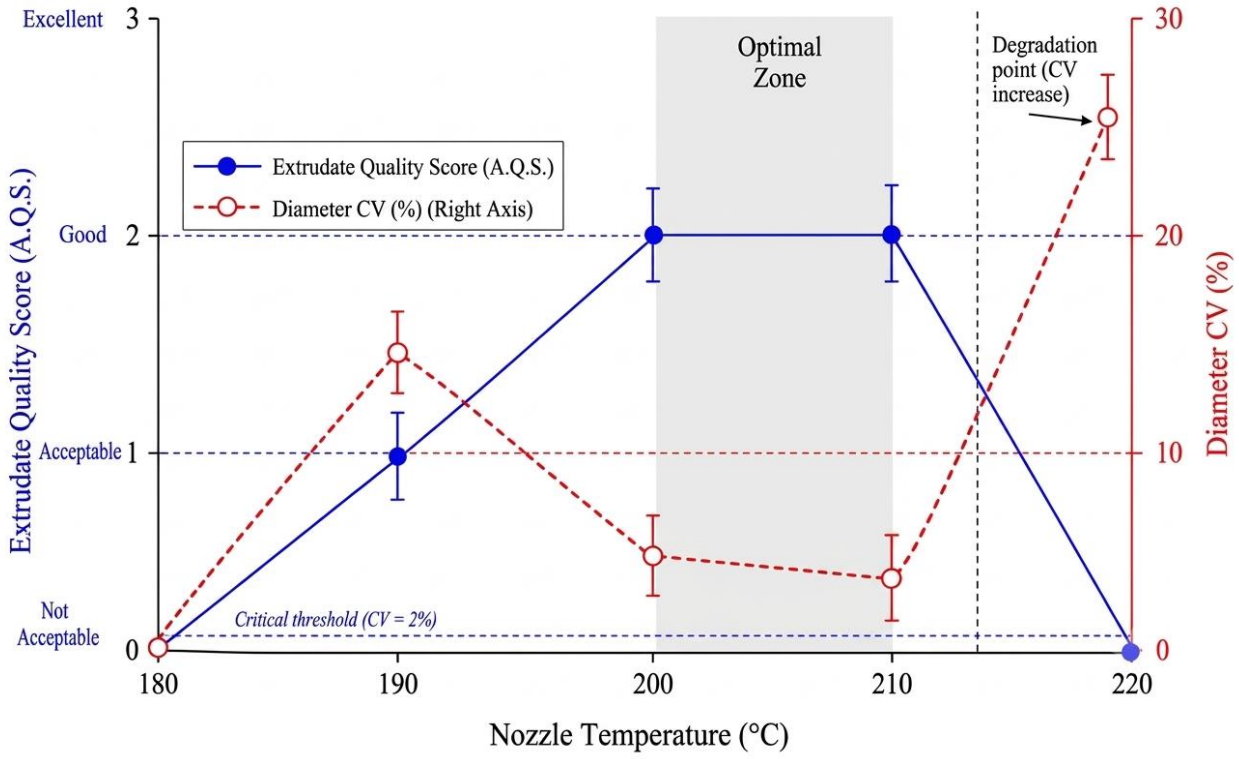


Fig. 6 Effect of nozzle temperature on extrudate quality score and filament diameter Coefficient of Variation (CV) during recycled pet extrusion

3.6. Comparison with Related Work and Limitations

The experimental results indicate that the proposed extrusion system performs competitively with previously reported laboratory-scale plastic recycling extruders while offering a simplified and cost-effective engineering configuration. Earlier studies have reported filament diameter Coefficients of Variation (CV) in the range of 8-15% for open-source recycled PET extrusion systems, whereas the incorporation of active haul-off mechanisms and closed-loop diameter control has reduced CV values to below 3% under optimized operating conditions. The present prototype achieved comparable within-trial diameter CV (3.9-5.2%, Table 4) during its steady-state trials, but the overall filament diameter remained below the 1.75 mm target and did not meet the ±0.05 mm commercial FDM tolerance, and downstream filament handling (rather than the extrusion process itself) was the main limiting factor for dimensional accuracy. This observation indicates that, although the mechanical structure and thermal regulation performed as intended, downstream filament handling exerted a greater influence on final product quality than the extrusion process itself.

Several limitations of the present study should be highlighted for the interpretation of these results and for planning future work. First, the structural FEA (Section 3.1, Table 2) considered only static weight and rated-torque loading; thermal stress, start-up/impact loading, weld fatigue and the temperature-dependent reduction in SS400 strength at elevated barrel-zone temperatures were not modeled. Second, all statistical analysis in this study is descriptive (mean, SD, CV) and based on a single laboratory session without randomized design, ANOVA, or independent replication across sessions (Section 2.5); the results should therefore be regarded as prototype characterization and preliminary parameter screening rather than a statistically validated process optimization. Third, the temperature screening (Section 3.5) is an empirical, qualitative assessment; the melt temperature, shear heating, die pressure and residence time were not independently measured, and the proposed 200-210°C working window and the thermo-oxidative degradation interpretation at 220°C have not been confirmed with quantitative material characterization (e.g., intrinsic viscosity, melt flow index, DSC, TGA). Fourth, the prototype does not incorporate an automatic haul-off unit or closed-loop laser diameter measurement, making filament dimensions susceptible to gravitational draw-down and manual winding variability. Fifth, and most directly relevant to the stated FDM application, no 3D-printing trials were performed with the filament produced by this system; the present results demonstrate that the prototype can produce continuous recycled PET extrudate, but they do not demonstrate reliable feeding, printing, or end-part quality in an actual FDM printer, and this validation is required before the system can be described as producing FDM-grade filament. Finally, the evaluation was limited to a single post-consumer PET feedstock under laboratory conditions, so the applicability of the system to other thermoplastics and to

continuous long-term production has not yet been established. Addressing these limitations, future work should integrate synchronized puller control with real-time diameter feedback, direct melt-temperature and post-processing material characterization, a randomized multi-session experimental design (e.g., factorial design or response-surface methodology) for genuine process optimization, and actual FDM printing trials to validate end-use filament performance. These developments would strengthen the capability of decentralized recycling systems to produce filament with the consistency required for commercial fused deposition modeling applications while preserving the low-cost philosophy of the present design.

4. Conclusion

This study describes the engineering design, fabrication, finite element assessment and experimental characterization of a lab-scale plastic extruder intended to recycle post-consumer PET into filament for potential Fused Deposition Modeling (FDM) applications. The proposed system integrates a mechanically robust structure, PID-based temperature control and a variable frequency drive, offering a practical and low-cost platform for decentralized plastic recycling. Static finite element analysis, under the weight and rated-torque loading described in Section 2.2, indicated that the mechanical strength of the structural design is adequate for these specific loading conditions: the predicted maximum von Mises stress remained well below the yield strength of SS400 structural steel, and all critical components had safety factors greater than five. This assessment did not include thermal stress, start-up/impact loading, weld fatigue, or elevated-temperature strength effects, and should be interpreted accordingly. In the extrusion-speed trials, the system reached a comparatively stable operating condition after excluding one trial with an unexplained excursion, giving a steady-state extrusion speed of 366.0 ± 23.1 cm min^{-1} (CV = 6.3%); the cause of the excluded trial's behavior was not conclusively established and warrants further replicated testing. The strong linear relationship between inverter frequency and screw rotational speed (R^2 = 0.999) further verified the effectiveness of the transmission system for predictable speed control. An empirical temperature screening across five nozzle setpoints indicated that nozzle temperatures of 200-210°C (with barrel temperature 20°C lower) gave the best extrudate quality and lowest dimensional variability among the conditions tested, while 220°C produced visibly degraded extrudate; however, this screening was qualitative, and the melt temperature, residence time, and post-processing material properties associated with these conditions were not independently measured or characterized, so this should be regarded as preliminary operating guidance rather than a validated thermal-degradation mechanism or optimum. Across all trials, filament diameter remained below the 1.75 mm target and did not meet the ±0.05 mm commercial FDM tolerance; downstream filament handling, rather than the extrusion process itself, was the main limitation for dimensional accuracy, and no 3D-printing trials were conducted to confirm end-use FDM performance. Future development should focus on the integration of synchronized haul-off control with closed-loop laser diameter monitoring, direct melt-temperature and post-processing material characterization, a randomized multi-session experimental design for rigorous process optimization, and actual FDM printing validation. To summarize, the developed extrusion system provides a preliminary, low-cost engineering basis for decentralized PET recycling and illustrates the potential of small-scale extrusion technology to contribute to circular manufacturing and sustainable plastic waste valorization, pending the further validation outlined above.

Beyond its engineering contributions, the proposed extrusion system supports sustainable manufacturing by enabling decentralized recycling of post-consumer PET into value-added products. The developed technology contributes to SDGs 9, 12, and 13 by promoting circular resource utilization, reducing plastic waste, and improving the sustainability of additive manufacturing supply chains.

Conflicts of Interest

The authors declare that there is no conflict of interest regarding the publication of this paper.

Funding Statement

This research received no external funding.

Acknowledgments

The authors gratefully acknowledge the Faculty of Engineering, Bangkok Thonburi University, for providing laboratory facilities and fabrication resources for this project. The authors also thank the advisors for their guidance throughout the design and testing phases.

References

[1] Roland Geyer, Jenna R. Jambeck, and Kara Lavender Law, "Production, use, and Fate of all Plastics ever Made," *Science Advances*, vol. 3, no. 7, pp. 1-5, 2017. [CrossRef] [Google Scholar] [Publisher Link]

[2] OECD, "Global Plastics Outlook: Economic Drivers, Environmental Impacts and Policy Options," *OECD Publishing*, 2022. [CrossRef] [Google Scholar] [Publisher Link]

[3] Jenna R. Jambeck et al., "Plastic Waste Inputs from Land into the Ocean," *Science*, vol. 347, no. 6223, pp. 768-771, 2015. [CrossRef] [Google Scholar] [Publisher Link]

[4] Maocai Shen et al., "(Micro)Plastic Crisis: Un-Ignorable Contribution to Global Greenhouse Gas Emissions and Climate Change," *Journal of Cleaner Production*, vol. 254, pp. 1-13, 2020. [CrossRef] [Google Scholar] [Publisher Link]

[5] Yanasinee Suma, Chongrak Polprasert, and Numfon Eaktasang, "Urban Waste Composition Associated with Online Food Delivery in Bangkok, Thailand, with Emphasis on Plastic Waste Management," *Urban Science*, vol. 10, no. 1, pp. 1-17, 2026. [CrossRef] [Google Scholar] [Publisher Link]

[6] Salita Kamsook et al., "Investigation of Plastic Waste Management in Thailand using Material Flow Analysis," *Waste Management and Research: The Journal for a Sustainable Circular Economy*, vol. 41, no. 4, pp. 924-935, 2023. [CrossRef] [Google Scholar] [Publisher Link]

[7] Luke Makarichi, Warangkana Jutidamrongphan, and Kingsley Okpara, "A Novel Approach to Characterizing Plastic Waste Releases from Land-based Sources using Material Flow Analysis: The Case of Thailand," *Waste Management and Research: The Journal for a Sustainable Circular Economy*, vol. 43, no. 12, pp. 2043-2055, 2025. [CrossRef] [Google Scholar] [Publisher Link]

[8] Sutisa Samitthiwetcharong et al., "Enhancing Circular Plastic Waste Management: Reducing GHG Emissions and Increasing Economic Value in Rayong Province, Thailand," *Heliyon*, vol. 10, no. 18, pp. 1-13, 2024. [CrossRef] [Google Scholar] [Publisher Link]

[9] Zoé O.G. Schyns, and Michael P. Shaver, "Mechanical Recycling of Packaging Plastics: A Review," *Macromolecular Rapid Communications*, vol. 42, no. 3, pp. 1-27, 2021. [CrossRef] [Google Scholar] [Publisher Link]

[10] Vincenzo Titone, Luigi Botta, and Francesco Paolo La Mantia, "Mechanical Recycling of New and Challenging Polymer Systems: A Brief Overview," *Macromolecular Materials and Engineering*, vol. 310, no. 1, pp. 1-13, 2025. [CrossRef] [Google Scholar] [Publisher Link]

[11] Mehran Namjoufar et al., "Overcoming Technical Barriers in Mechanical Recycling of Plastic Waste: The Role of Engineered Additives," *Journal of Environmental Chemical Engineering*, vol. 14, no. 2, pp. 1-41, 2026. [CrossRef] [Google Scholar] [Publisher Link]

[12] Chiara Fiorillo et al., "Molecular and Material Property Variations during the Ideal Degradation and Mechanical Recycling of PET," *RSC Sustainability*, vol. 2, no. 12, pp. 3596-3637, 2024. [CrossRef] [Google Scholar] [Publisher Link]

[13] Yong-Chul Jang et al., "Recycling and Management Practices of Plastic Packaging Waste towards a Circular Economy in South Korea," *Resources, Conservation and Recycling*, vol. 158, pp. 1-11, 2020. [CrossRef] [Google Scholar] [Publisher Link]

[14] Atiq Uz Zaman, "A Comprehensive Study of the Environmental and Economic Benefits of Resource Recovery from Global Waste Management Systems," *Journal of Cleaner Production*, vol. 124, pp. 41-50, 2016. [CrossRef] [Google Scholar] [Publisher Link]

[15] Qin Chen et al., "Green Economic Value Analysis and Environmental Evaluation of Modified Rubber Concrete," *International Conference on Energy Engineering and Environmental Engineering*, Springer, Cham, pp. 251-263, 2026. [CrossRef] [Google Scholar] [Publisher Link]

[16] Christian Baechler, Matthew DeVuono, and Joshua M. Pearce, "Distributed Recycling of Waste Polymer into RepRap Feedstock," *Rapid Prototyping Journal*, vol. 19, no. 2, pp. 118-125, 2013. [CrossRef] [Google Scholar] [Publisher Link]

[17] Aubrey L. Woernne et al., "RepRapable Recyclebot: Open Source 3-D Printable Extruder for Converting Plastic to 3-D Printing Filament," *HardwareX*, vol. 4, pp. 1-58, 2018. [CrossRef] [Google Scholar] [Publisher Link]

[18] Ali Kassab et al., "Advancing Plastic Recycling: Challenges and Opportunities in the Integration of 3D Printing and Distributed Recycling for a Circular Economy," *Polymers*, vol. 15, no. 19, pp. 1-45, 2023. [CrossRef] [Google Scholar] [Publisher Link]

[19] Mohamed Hassanien et al., "A Low-Cost Process for Fabricating Reinforced 3D Printing Thermoplastic Filaments," *Polymers*, vol. 15, no. 2, pp. 1-19, 2023. [CrossRef] [Google Scholar] [Publisher Link]

[20] Carolina Cardona, Abigail H. Curdes, and Aaron J. Isaacs, "Effects of Filament Diameter Tolerances in Fused Filament Fabrication," *The Indiana University Journal of Undergraduate Research*, vol. 2, no. 1, pp. 44-47, 2016. [CrossRef] [Google Scholar] [Publisher Link]

[21] Mohamed Refat et al., "Investigation of the Influence of Manufacturing on Filament Production and its Impact on Additive Manufactured Structures," *Polymers*, vol. 17, no. 5, pp. 1-18, 2025. [CrossRef] [Google Scholar] [Publisher Link]

[22] Volker Schöppner, and Verena Resonnek, "Investigation of the Barrel Temperature Profile on the Process Behavior of Single Screw Extruders and Strategies to Determine the Optimal Temperature Control," *AIP Conference Proceedings*, vol. 2139, no. 1, pp. 1-6, 2019. [CrossRef] [Google Scholar] [Publisher Link]

[23] Ola Rashwan et al., "Extrusion and Characterization of Recycled Polyethylene Terephthalate (rPET) Filaments Compounded with Chain Extender and Impact Modifiers for Material-Extrusion Additive Manufacturing," *Scientific Reports*, vol. 13, no. 1, pp. 1-15, 2023. [CrossRef] [Google Scholar] [Publisher Link]

[24] Saurabh Kausadikar et al., "Design and Analysis of Single Screw Extruder for Hybrid Manufacturing Process," *Advances in Manufacturing, Automation, Design and Energy Technologies*, Springer, Singapore, pp. 397-407, 2023. [CrossRef] [Google Scholar] [Publisher Link]

[25] X.Z. Zhu et al., "Study of Dynamic Flow and Mixing Performances of Tri-Screw Extruders with Finite Element Method," *Advances in Mechanical Engineering*, vol. 5, pp. 1-12, 2013. [CrossRef] [Google Scholar] [Publisher Link]

[26] Janko Petrovčič, and Damir Vrančić, *Temperature Control in a Plastic Extruder Control System*, Case Studies in Control, Springer, London, pp. 157-183, 2013. [CrossRef] [Google Scholar] [Publisher Link]

[27] Shubham Sadhya et al., "Development of Lab-Scale Extruder to Produce Feedstock Filament for 3D Printing using Recycled Thermoplastics," *Materials Today: Proceedings*, vol. 80, no. 1, pp. 150-155, 2023. [CrossRef] [Google Scholar] [Publisher Link]

[28] Sathish Kumar Adapa, and Jagadish, "Design and Fabrication of Internal Mixer and Filament Extruder for Extraction of Hybrid Filament Composite for FDM Applications," *International Journal on Interactive Design and Manufacturing*, vol. 18, no. 1, pp. 419-432, 2024. [CrossRef] [Google Scholar] [Publisher Link]